



## BUOYANCY EFFECT STUDY ON CONVECTIVE ENHANCEMENT FOR VARIOUS BASE NANOFUIDS IN AN ENCLOSURE

Salah Mahdi salih  
salahmahditech@yahoo.com

Tahsin ali Husain  
tahosain2@gmail.com

Alforat Al Awsat Technical College/Al-Najaf Technical College/Auto. Eng. Dept.

### ABSTRACT

Buoyancy-driven heat transfer convection enhancement in a two-dimensional enclosure, for two cases boundary conditions: (isothermal and linearly varying) temperature differential heated walls utilizing Nano fluid is studied numerically. In this study, three various base fluids (water, ethylene glycol, or oil) based with (CuO) nanoparticles are tested. Calculations of heat transfer rates were accomplished for a range of Rayleigh number ( $10^3 \leq Ra \leq 10^6$ ), Prandtl number is taken as ( $Pr = 6.7, 204, \text{ and } 10959$ ), and solid volume fraction ( $0\% \leq \phi \leq 10\%$ ). Numerical computations are carried out for different combinations of relevant parameters involved in the study. Results showed that the heat transfer rate increases by increasing the volume fraction of the Nano fluid for all types of base Nano fluid considered. The increment in average Nusselt number is strongly dependent on the basic fluid and boundary condition chosen. The heat transfer rate also increases with increases of Rayleigh number, and Prandtl number. Based on the present results, oil-base nanoparticle in an enclosure with the isothermal temperature walls is preferable to attain overall heat transfer enhancement. Also, the enhancement in heat transfer with (0.1) solid volume fraction of (CuO) particles based with different basic fluids such as (water, EG, or oil) increases (26.7%, 28.8%, and 32.94%) respectively for low (Ra) as compared to the base fluid. For verification of current study, the results have been compared with the recent studies at the same boundary conditions and are a good agreement.

**KEYWORDS :** - Buoyancy effect; Convective enhancement; various bases Nano-fluid.

### دراسة تأثير قوة الطفو على تحسين الحمل الحراري لموائع نانوية مختلفة لمحتوى مغلق

د. تحسين علي حسين م. صلاح مهدي صالح

جامعة الفرات الاوسط التقنية

الكلية التقنية الهندسية - نجف / قسم هندسة تقنيات السيارات

الخلاصة :-

تم إجراء دراسة عددية لتحسين الحمل الحراري الطبيعي لمحتوى مغلق ثنائي البعد، لحالتين من الظروف الحدية مختلفة: (منتظمة، متغيرة خطياً) لدرجة حرارة الجدران المسخنة بشكل متباين باستخدام مائع نانوي. في هذه الدراسة، تم اختبار ثلاث مواد سائلة أساسية (الماء، أثيلين كلاًيكول، والزيت) موضوعة مع جسيمات دقيقة جداً لمسحوق (أكسيد النحاس). تم تمثيل النتائج العددية لمعدلات انتقال الحرارة لعدد رالي في المدى ( $10^3 \leq Ra \leq 10^6$ )،

التركيز الحجمي ( $0\% \leq \phi \leq 10\%$ ) ، إخذ عدد برانتل ( $Pr=6.7, 204, \text{ and } 10959$ ). المحاكاة العددية تضمنت أختبار مختلف العوامل المتعلقة بالدراسة. النتائج بينت ان معدل انتقال الحرارة يزداد بزيادة التركيز الحجمي للمائع النانوي لجميع المواد السائلة المدروسة . الزيادة بمعدل عدد نسلت تكون معتمدة بشكل قوي على نوع المادة السائلة الأساسية والظرف الحدي المختار. كذلك معدل انتقال الحرارة يزداد بزيادة عدد رالي و عدد برانتل. على اساس النتائج الحالية ، تبين إن سائل الزيت الموضوع للجسيمات الدقيقة لمحتوى مغلق ذات درجة حرارة منتظمة للجدران هي افضل حالة للحصول على اكبر زيادة لانتقال الحرارة. كذلك، تحسين معدل انتقال الحرارة بتركيز حجمي ( $\phi = 0.1$ ) و لمسحوق أكسيد النحاس موضوع مع مواد سائلة مختلفة مثل (الماء، أنثيلين كلايكون، والزيت) هو (26.7%، 28.8%، 32.94%) and على التوالي ولعدد رالي واطيء. وللتحقق من النموذج الحالي، تم مقارنة النتائج العددية للدراسة الحالية مع دراسات سابقة عند نفس الظروف الحدية وكانت مقبولة.

الكلمات الدالة: تأثير قوة الطفو ، تحسين انتقال الحرارة بالحمل ، موائع نانوية مختلفة

## NOMENCLATURE

g	gravitational acceleration ( $\text{ms}^{-2}$ )	$\omega$	vorticity ( $\text{s}^{-1}$ )
H	enclosure height (m)	$\Omega$	dimensionless vorticity
H	heat transfer coefficient ( $\text{W}/\text{m}^2 \text{K}$ )	$\psi$	dimensional stream function ( $\text{m}^2\text{s}^{-1}$ )
L	enclosure width (m)	$\Psi$	dimensionless stream function
P	pressure (Pa)	$\rho$	density ( $\text{kg m}^{-3}$ )
T	temperature (K)	$\mu$	dynamic viscosity ( $\text{kg m}^{-1}\text{s}^{-1}$ )
u, v	dimensional velocity componente	<u>Subscripts</u>	
U, V	dimensiones velocity componentes	co	cold nf nanofluid
x, y	dimensional Cartesian coordinantes	eff	effective s nanoparticle
X, Y	dimensionless Cartesian coordinates	f	fluid
<u>Greek Symbols</u>		ho	hot
$\beta$	thermal expansion coefficient ( $\text{K}^{-1}$ )		
$\phi$	solid volume fraction		
$\nu$	kinematic viscosity ( $\text{m}^2 \text{s}^{-1}$ )		
$\theta$	dimensionless temperature		

## INTRODUCTION:

Nano Fluids are used for heat transfer convection in many types of equipment. The metallic or non-metallic particles of higher thermal conductivity with dimensions less than (100 nm) such as (Cu, Ag,  $\text{AL}_2\text{O}_3$ , CuO, and  $\text{TiO}_2$ ) are dispersed in conventional heat transfer basic fluids such as oil, water, ethylene glycol (EG), propylene glycol, to provide enhanced heat transfer characteristics due to their increased effective thermal conductivity, **Xuan et al.(2003)**. Because of their Nano fluids have excellent thermal performance are used in industrial engineering applications such as: heat exchangers, solar collector plants, and vehicle cooling fluids, oils, and lubricants.

Firstly, Nano fluids model in an enclosure was proposed by (**Khanafar et al., 2003**) and the authors studied the effect of free convection on the energy enhancement. The results showed that the Nusselt number with Nano fluid increases by increasing in the volume fraction of nanoparticle. (**Tiwari et al., 2007**) reported a single-phase model, in which solid particles are considered to behave as fluids, because the nanoparticles are easy fluidized.

The effect of water-based  $AL_2O_3$  Nano fluids in a rectangular cavity on the buoyancy-driven heat transfer is investigated, by (Hwang et al., 2007). They showed that the average of heat transfer coefficient enhancement is decreased as increases the size of nanoparticles.

(Jou et al., 2007) utilized Nano fluids to enhance natural convection heat transfer in a rectangular enclosure. They indicated that volume fraction of nanofluids cause an increase in the average heat transfer coefficient. (Lin et al., 2010) analyzes the heat transfer and fluid flow of natural convection in a cavity filled with  $AL_2O_3$  -water Nano fluid that operates under differentially heated walls. They showed that the decreasing in the Prandtl number results in amplifying the effects of nanoparticles due to increased effective thermal diffusivity. A numerical study of the natural convection of Cu–water Nano -fluid in a cavity with partially active side walls is conducted by, (Sheikhzadeh et al., 2011). They showed the average Nusselt number increases with increasing both the Rayleigh number and the volume fraction of the nanoparticles.

Buoyancy-driven heat transfer convection in an enclosure utilizing nanofluids is studied to consider the natural convection heat and fluid flow characteristics in a square enclosure with two cases: isothermal, and linearly varying hot-wall temperature. In this study, three basic fluids (water, ethylene glycol (EG), or oil) based Nano fluid containing of (CuO) nanoparticle are tested to investigate the effect of (nanoparticles solid volume fraction ( $\phi$ ), boundary condition of hot wall, Rayleigh number (Ra), and the effects of base Nano fluid on heat and flow fields.

## MATHEMATICAL FORMULATION

Consider a steady state two-dimensional of enclosure filled with nanofluid. In the present problem, the mathematical equations describing the physical model are based on the following assumptions:

- I. The base fluids (water, EG, and oil engine) and the nanoparticle (CuO) are in thermal equilibrium.
- II. The thermophysical properties of the nanofluid are assumed constant except for a variation of the density which is determined based on Boussinesq approximation.
- III. The nanofluid flow in the enclosure is Newtonian, incompressible and laminar.
- IV. Radiation heat transfer between the sides of the enclosure is negligible when compared with the other mode of heat transfer.

The thermophysical properties of the basic fluids and the nanoparticle are presented in **Table 1**. The geometric and the Cartesian coordinate system are schematically shown in **Fig. 1**.

Under the above assumptions, for natural convection in a square enclosure, the fluid and thermal fields are governed by the dimensionless equations of stream function, vorticity transport and energy. These may be written in the form: (Ayad et al., 2011)

$$\left( \frac{\partial^2 \Psi}{\partial X^2} + \frac{\partial^2 \Psi}{\partial Y^2} \right) = -\Omega \quad (1)$$

$$\frac{\partial \Psi}{\partial Y} \frac{\partial \Omega}{\partial X} - \frac{\partial \Psi}{\partial X} \frac{\partial \Omega}{\partial Y} = a1 \left( \frac{\partial^2 \Omega}{\partial X^2} + \frac{\partial^2 \Omega}{\partial Y^2} \right) + a2 \frac{\partial \theta}{\partial X} \quad (2)$$

$$a1 = \text{Pr} / \left( (1 - \phi)^{2.5} \left( (1 - \phi) + \phi \frac{\rho_s}{\rho_f} \right) \right)$$

Where:

$$a2 = \text{Ra Pr} \left[ \frac{1}{\frac{(1 - \phi) \rho_f}{\phi \rho_s} + 1} \frac{\beta_s}{\beta_f} + \frac{1}{\frac{\phi \rho_s}{(1 - \phi) \rho_f} + 1} \right]$$

$$\frac{\partial \theta}{\partial X} \frac{\partial \Psi}{\partial Y} - \frac{\partial \theta}{\partial Y} \frac{\partial \Psi}{\partial X} = \lambda \left( \frac{\partial^2 \theta}{\partial X^2} + \frac{\partial^2 \theta}{\partial Y^2} \right) \quad (3)$$

Where:

$$\lambda = \left[ \frac{k_{nf}/k_f}{(1 - \phi) + \phi \frac{(\rho c_p)_s}{(\rho c_p)_f}} \right]$$

The components velocities respectively are:

$$u = \frac{\partial \psi}{\partial y}, \quad v = -\frac{\partial \psi}{\partial x} \quad (4)$$

The effective density of a fluid containing suspended particles is given by:

$$\rho_{nf} = (1 - \phi) \rho_f + \phi \rho_s \quad (5)$$

The heat capacitance of the Nano -fluid is expressed as, (**Fusegi T. et al., 1991**), and (**Ho et al., 2008**):

$$(\rho c_p)_{nf} = (1 - \phi) (\rho c_p)_f + \phi (\rho c_p)_s \quad (6)$$

The effective thermal conductivity of the Nano -fluid is approximated by the Maxwell–Garnetts model: (**Ho et al., 2008**); and (**Aminossadati et al., 2009**).

$$k_{eff} = \frac{k_{nf}}{k_f} = \frac{k_s + 2k_f - 2\phi(k_f - k_s)}{k_s + 2k_f + \phi(k_f - k_s)} \quad (7)$$

Moreover, the effective dynamic viscosity of the Nano fluid which is given by (**Brinkman, 1952**):

$$\mu_{nf} = \frac{\mu_f}{(1 - \phi)^{2.5}} \quad (8)$$

The following dimensionless groups based on length of enclosure (L) are introduced:

$$\begin{aligned}
 X &= \frac{x}{L}; \quad Y = \frac{y}{L}; \quad \Omega = \frac{\omega L^2}{\alpha_f}; \quad \Psi = \frac{\psi}{\alpha_f}; \quad U = \frac{uL}{\alpha_f}; \quad V = \frac{vL}{\alpha_f}; \\
 \theta &= \frac{T - T_{co}}{T_{ho} - T_{co}}; \quad Ra = \frac{g\beta_f\rho_f(T_{ho} - T_{co})L^3}{\mu_f\alpha_f}; \quad Pr = \frac{\mu_f}{\rho_f\alpha_f}
 \end{aligned}
 \tag{9}$$

**BOUNDARY CONDITIONS**

The governing equations of nanofluid are nonlinear and coupled partial differential equations must be solved by using appropriate boundary conditions. In this study, the horizontal walls of an enclosure are insulated for two cases of boundary conditions:

**I- Case.1:** The vertical walls are differentially heated, isothermally at (T<sub>ho</sub>) and (T<sub>co</sub>) respectively, (T<sub>ho</sub> > T<sub>co</sub>).

**II- Case.2:** The left vertical wall of the enclosure is heated linearly with height (T<sub>ho</sub> = f(y)), while the right vertical wall is cooled at a constant temperature (T<sub>co</sub>). No slip boundary conditions are applied on the enclosure walls for two cases, as shown in **Fig.1**.

**The dimensionless form of the boundary conditions is given by:**

1- On the left wall (hot) for X = 0; 0 ≤ Y ≤ 1

a- Bc.s of stream function and vorticity are:

$$\Psi = 0; \quad \Omega = -\frac{\partial^2\Psi}{\partial X^2} = \frac{3(\Psi_1 - \Psi_2)}{\Delta X^2} - \frac{\Omega_2}{2}$$

b- Bc.s of temperature is:

$$\theta = 1 \quad \text{for case1}$$

$$\theta = Y \quad \text{for case2}$$

2- On the right wall (cold) for X = 1; 0 ≤ Y ≤ 1

a- Bc.s of stream function and vorticity are:

$$\Psi = 0; \quad \Omega = -\frac{\partial^2\Psi}{\partial X^2} = \frac{3(\Psi_m - \Psi_{m-1})}{\Delta X^2} - \frac{\Omega_{m-1}}{2}$$

b- Bc.s of temperature is:

$$\theta = 0 \quad \text{for case1}$$

$$\theta = 0 \quad \text{for case2}$$

3- On the top and bottom walls

a- at top wall insulated for Y = 1; 0 ≤ X ≤ 1

$$\Psi = 0; \quad \Omega = -\frac{\partial^2\Psi}{\partial Y^2} = \frac{3(\Psi_n - \Psi_{n-1})}{\Delta Y^2} - \frac{\Omega_{n-1}}{2}; \quad \frac{\partial\theta}{\partial Y} = 0$$

b- At bottom wall insulated for Y = 0; 0 ≤ X ≤ 1

$$\Psi = 0; \quad \Omega = -\frac{\partial^2\Psi}{\partial Y^2} = \frac{3(\Psi_1 - \Psi_2)}{\Delta Y^2} - \frac{\Omega_2}{2}; \quad \frac{\partial\theta}{\partial Y} = 0$$

(10)

(11)

The local variation of the Nusselt number of the fluid can be expressed as:

$$Nu_y = \frac{hL}{k_f} \quad (12)$$

The local heat transfer coefficient is expressed as:

$$h = \frac{q_w}{(T_{ho} - T_{co})} \quad (13)$$

The thermal conductivity is expressed as:

$$k_{nf} = -\frac{q_w}{\partial T / \partial x} \quad (14)$$

By substituting **Eqs. (13, 14, and 7)** into **Eq. (12)**, and using the dimensionless quantities, the local Nusselt number ( $Nu_y$ ) on the left wall is written as:

$$Nu_y = -\left(\frac{k_{nf}}{k_f}\right) \partial \theta / \partial X \quad (15)$$

The heat transfer rate at the hot wall of the enclosure is presented by means of the Nusselt number ( $Nu$ ), which is evaluated as follows:

$$Nu = \int_0^1 Nu_y dY \quad (16)$$

A 1/3rd Simpson's rule of integration is used to evaluate **Eq. (16)**.

The heat transfer is enhanced with an addition of nanoparticles. To estimate the enhancement of the heat transfer in the case of (CuO) Nano fluid and in the case of pure fluid ( $\phi = 0\%$ ), the enhancement is defined:

$$\varepsilon = \frac{Nu_\phi - Nu_{\phi=0\%}}{Nu_{\phi=0\%}} \times 100\% \quad (17)$$

## NUMERICAL METHOD AND VALIDATION:

The dimensionless governing **Eqs. (1 to 3)** with the boundary conditions **Eqs. (10)** and **(11)** were analysed by utilizing a finite difference scheme. Suppose a two-dimensional region covered with a square mesh as is shown in **Fig.2**. The mesh size which consists of ( $m$ ) horizontal and ( $n$ ) vertical lines positioned at intervals of ( $\Delta x$ ) and ( $\Delta y$ ), respectively. For simplicity, assumed that both increments ( $\Delta x$ ), and ( $\Delta y$ ) are constant. **Table 2** shows an accuracy test using the finite difference method using five sets of grids:( 51×51, 61×61, 71×71, 81×81, and 91×91). There is a good agreement found between (71×71) to (91×91) grids. Therefore, a (81×81) grid is chosen to calculate the flow and heat transfer behavior over the range of operational parameter values considered.

To ensure the accuracy and validity of the current model, a system composed of pure fluid in an enclosure analysis with ( $Pr = 6.7$ ), and different ( $Ra$ ) numbers. This system has been studied by other research groups, including (**Markatos et al., 1984**), (**Fusegi et al., 1991**), (**Khanafar et al., 2003**), (**Tiwari et al., 2007**), (**lin et al., 2010**), and (**Sheikhzadeh et al., 2011**); **Table 3** shows a comparison between the obtained results of the current study and the values presented in the literature. The quantitative comparisons for the average Nusselt numbers along the hot wall indicate a good agreement, as shown in **Fig.3**.

In this study, the numerical methods were used central difference quotients to approximate the second derivatives in both the ( $X$ , and  $Y$ ) directions. And to get a stable

and converged solution for vorticity and energy equations, a forward– backward technique was used for uniformly grid distributed. The solution procedure starts by supplying initial guesses of the stream function, vorticity and temperature then computes a converged solution by a Gauss–Seidel iteration technique. The sequence of numerical steps based on finite difference is as follow, (Najdat, 1987):

1. Initialize the stream function, vorticity, and temperature fields ( $\Psi$ ,  $\Omega$ , and  $\theta$ ).
2. Establish suitable boundary conditions;
3. Solve Eqs. (1) and (2) for  $\Psi$  and  $\Omega$ .
4. Solve Eq. (3) for  $\theta$ .
5. Check Eq. (18) for convergence, if it is satisfied, calculations will be ended. Otherwise, replace ( $\Psi$ ,  $\Omega$ , and  $\theta$ ) and return to step (2) and repeat the above procedure until convergence is achieved:

$$\tau = \frac{\sum_{i=1}^{i=M} \sum_{j=1}^{j=N} |\zeta^{r+1}_{i,j} - \zeta^r_{i,j}|}{\sum_{i=1}^{i=M} \sum_{j=1}^{j=N} |\zeta^{r+1}_{i,j}|} \leq 10^{-5} \quad (18)$$

Where ( $\tau$ ) is the tolerance; (M, and N) are the number of grid points in the (x, and y) directions, respectively, and ( $\zeta$ ) stands for ( $\Psi$ ,  $\Omega$  or  $\theta$ ); ( $r$ ) denotes the iteration step.

The numerical method was implemented in a **Fortran Power Station 4.0** language program was built to execute the numerical algorithm which is mentioned above. It is a general for a natural convection enhancement in a two-dimensional enclosure by utilizing various nanofluids, as shown in the flow chart **Fig. (4)**.

## RESULTS AND DISCUSSION

In this section, numerical computations are carried out and performed to show the effect of the physical parameters on the resulting streamlines and isotherms contours as well as local and average Nusselt number along the hot wall and velocity profiles. The results of this study are shown in **Figs. (5-14)**. In this study was taken as ( $Ar = 1$ ) square enclosure, for a range of Rayleigh number ( $10^3 \leq Ra \leq 10^6$ ), Prandtl number is taken as ( $Pr = 6.7, 204, \text{ and } 10959$ ) of basic fluids such as : (water, ethylene glycol (EG), and oil) respectively, created with (CuO) nanoparticle range of solid volume fraction ( $0\% \leq \phi \leq 10\%$ ).

**Figures (5 and 6)** (a)- (d) show a comparison between (CuO-oil) Nano fluid is plotted by dashed lines, and pure fluid is plotted by solid lines for streamlines and isotherms: case1, and case2. The different values of Rayleigh number (Ra) show effect of the (Ra) on the contours for streamlines and isotherms of enclosure filled with Nano fluid at ( $\phi = 4\%$ ) for both Nano fluid and pure fluid (water) of two cases. A larger absolute value of the stream function is identified for the Nano fluid as compared to the pure water, representing that the strength of circulation increases with an increasing particle volume fraction at a particular Rayleigh number, the minimum value of stream function changes from ( $-1.36$  to  $-20$ )<sub>case1</sub> at ( $Ra = 10^3, 10^4, 10^5, \text{ and } 10^6$ ), respectively. For a low Ra number, the isotherm is almost vertical since heat is transferred by conduction between the hot and cold walls. In addition, with the use of a Nano fluid, the lesser temperature gradient at the heated surface as compared to the use of pure water due to the development of thermal boundary thickness is disclosed, see **Fig.5 (a-d)**.

**Figure (6)** shows the flow pattern as a single cell inhabiting the whole enclosure. The core region of the cell is at the middle of the enclosure when ( $Ra = 10^3$ ). The core region of the Nano fluid is reduced as compared to pure fluid for all values of Ra number, the minimum

value of stream function changes from  $(-0.71 \text{ to } -12.5)_{\text{case2}}$  at  $(Ra = 10^3, 10^4, 10^5, \text{ and } 10^6)$ , respectively. When the Ra number increases, the core region of the cell changes towards the cold wall and lengthens. The core region of the enclosure, it is clear that the flow strength and the temperature isotherms are influenced by the being there of nanoparticles. For lower values of (Ra) number, the flow strength is higher for (CuO) than pure fluid oil. The core region moves towards the top-right corner of the enclosure when  $(Ra = 10^6)$ . The isotherms cluster along the thermally active walls due to stronger circulation appears for both horizontal and vertical fluid layer. For higher Ra numbers, natural convection become more dynamic and the fluid moves faster and the isotherms become more overflowing next to adiabatic walls. See **Fig. 6(a-d)**, case2.

The effect of the solid volume fraction on the streamlines and isotherms of (CuO-oil) Nano fluid at  $(Ra = 10^5)$  for case2, as shown in **Fig. (7)**. It is clear that, the fluid moves from left towards right and forms a clockwise circular cell with  $(\Psi_{\text{min}} = -7.5)$  at  $(\phi = 2.5\%)$ . Also, at the left wall of the enclosure is presented of a heat source helps the cell to stretch vertically beside position of the linearly varying heat source. By increasing in solid volume fraction causes in a decreasing the intensity of buoyancy and hence the flow intensity so that, the minimum value of stream function changes from  $(-8 \text{ to } -9)$  at  $(\phi = 5\%, \phi = 0.1)$ , respectively. The actions of particles become irregular and random due to increasing of energy exchange rates in the fluid. Isotherms show that temperature gradients near the hot and cold walls become more severe. For  $(\phi = 0.025 \text{ to } 0.1)$ , the streamlines elongate parallel to the horizontal wall for pure fluid, see from Fig. 4(a-d).

**Figure (8 a-c)** shows a comparison between (CuO-water), (CuO-EG), and (CuO-oil) Nano fluid and pure fluid, case1 at  $(Ra = 10^5, \text{ and } \phi = 4\%)$  for different basic fluids such as (water, EG, and oil). It is observed that, the fluid follows of the enclosure by forming one clockwise circular cell for all basic fluids. Elongated shaped circulation cell is formed due to enclosure heated from the left corner. As the basic fluid changes, the flow rates at the centers of circulation increase and the core region of the cell moves towards the cold wall and elongates, the flow strength increases and the boundary layers become more illustrious for (CuO-water) Nano fluid, but the flow strength is higher for (CuO-oil) than (CuO-EG), and (CuO-water) Nano fluid, respectively.

**Figure (8 b-c)** shows the temperature drops slowly from the left wall at the isothermally heat source to the cold right wall. The corresponding isotherms display the higher characteristics of conduction for base fluid ethylene glycol than water with nanoparticles. This behavior is clear that the flow strength and the temperature isotherms are influenced by the being there of basic fluid. The variation of local Nusselt number is illustrated along the heated wall in **Fig.(9a)** using (CuO-oil) nanoparticles for different solid volume fraction at  $(Ra = 10^5)$ , case1. The values of local Nusselt number have higher values at onset of isothermal heating wall due to high temperature difference. Again, the highest local Nusselt number values were formed for high  $(\phi = 0.1)$  and the lowest one for low  $(\phi = 0\%)$ .

**Figure (9b)** shows a comparison of local Nusselt number is conducted inside a thermal enclosure with isothermal vertical walls at  $(Ra = 10^4, \phi = 6\%)$  for (CuO-water), (CuO-EG), and (CuO-oil) Nano fluid and demonstrates the effect of basic fluid on the local heat transfer rate of the enclosure. It is clearly, the local heat transfer rate for basic fluid water is lowest value as compared to those at the basic fluids EG, and oil has the highest local Nusselt number, respectively. This is because oil has the highest dynamic viscosity matched to other base fluids and (CuO) particle mixed properly in oil which contributes to increase the thermal transport capacity of the mixture. To show that nanofluids behave more like a fluid than the conventional particle –fluid mixture, a comparison of the isotherm and the velocity profiles is conducted inside a thermal enclosure with isothermal

vertical walls at various boundary conditions for two cases of (CuO-oil) nanofluids, as shown in **Fig. (10)**.

The effect of boundary conditions and the volume fraction ( $\phi$ ) on the isotherms and the velocity profiles at the mid-sections of the square enclosure are illustrated. The numerical results of the present study indicate that the heat transfer feature of a Nano fluid increases with the volume fraction of nanoparticles. The isotherms in Figure show that the vertical stratification of the isotherms breakdown with the linearly varying boundary condition as compared to this at the isothermal boundary condition. See **Fig. (10a)**. In addition, the vertical velocity at the center of the enclosure for isothermal boundary condition is very large compared with this at the linearly varying boundary condition where the fluid is moving at higher velocities. This behavior is also present for a single-phase flow. As the volume fraction increases, the velocity components of Nano fluid increase as a result of an increase in the energy transport through the fluid. Velocity heights of the vertical velocity component are shown in this figure at high ( $\phi$ ) for case1. The effect of an increase in the volume fraction on the velocity and temperature gradients along the centerline of the enclosure is shown in **Fig. (10b)**. **Figure (11)** shows a comparison of the vertical velocity sketches is conducted inside a thermal enclosure with linearly varying temperature vertical walls at ( $Ra=10^3$ , and  $10^5$ ) for different solid volume fraction ( $\phi$ ) of (Cu-oil) Nano fluid and demonstrates the effect of ( $Ra$ ), and the ( $\phi$ ) of nanoparticle on the velocity profiles at the mid-sections of the enclosure. The maximum y-velocity increases when the  $Ra$  number increases due to the strong buoyant flows, and it increases when the solid volume fraction ( $\phi$ ) increases due to the influence of the particle suspension effects on the convective flows. The effect of the ( $\phi$ ) on the y-velocity sketch is more important at  $Ra=10^5$  as compared to this at  $Ra=10^3$ , where the convective flow field is very strong and can be influenced by the particle suspension affects.

As the volume fraction ( $\phi$ ) increases (0) pure fluid to (0.1) Nano fluid, the velocity components of Nano fluid increases as a result of an increase in the energy transport through the fluid. High velocity peaks of the vertical velocity component are presented in this figure at high ( $\phi$ ) at  $Ra=10^5$ . The effect of an increase in ( $Ra$ ) and ( $\phi$ ) on the velocity along the centerline of the enclosure is shown in **Fig.(11a - b)**. **Figure (12)** displays the effects of  $Ra$  number on the average Nusselt number along the heat source for different solid volume fraction ( $\phi$ ) of (CuO-H<sub>2</sub>O) Nano fluid, and different boundary condition (isothermal, and linearly varying) temperature, respectively. The figure shows that the heat transfer rate increases practically with increasing the ( $Ra$ ), and ( $\phi$ ) Nano fluid, because of the decrease in an activity for both a fluid motion and its temperature. The lowest heat transfer rate was gained for pure fluid due to the conduction heat transfer. The highest heat transfer rate is verified when using Cu-water Nano fluid with isothermal as compared to this at the linearly varying boundary condition, see **Fig. (12a - b)**.

**Figure (13)** shows the comparison of average Nusselt numbers with solid volume fraction for CuO-water for different ( $Ra$ ) numbers ( $10^4$ , and  $10^6$ ). The results obviously indicate that ( $Nu$ ) increases with an increasing in ( $Ra$ ) numbers ( $10^4$  to  $10^6$ ) where the heat transfer is conduction dominated, the distribution of ( $Nu$ ) is completely linear. The distribution of the average Nusselt number becomes increasingly with the support of the convective transport in the isothermal (case1) of lower and higher values of ( $Ra$ ) as compared to this at the linearly varying (case2) of boundary condition due to its lowest temperature distribution for all solid volume fractions of (CuO) nanoparticles.

In addition, the effects of the solid volume fraction on the average Nusselt number and percentage heat transfer enhancement can be well arranged by studying the values offered in **Table 4**. This table presents the effect of  $f$  on ( $Nu$ ) and its relative increase percentage. For the case1, the results show that the effects of ( $\phi$ ) are clearer at low  $Ra$  number where

heat transfer is mainly due to conduction. As seen in this table, there exists major difference between isothermal and linearly varying temperature mainly for the ( $\phi=2.5\%$ ). This difference directly causes a discrepancy in the related (Nu) values. In compare, for the case2, the effects of  $f$  are more visible at high Ra numbers where convection is the main heat transfer mechanism.

Finally, the effect of different types of base fluids on the heat transfer rate versus the ( $\phi$ ) at ( $Ra=10^4$ ) for case1, is presented in **Fig. (14)**. to demonstrates the heat transfer efficacy of the Nano fluid. It can clearly be seen from this figure that (CuO-H<sub>2</sub>O) has the lowest value of the heat transfer rate while (CuO-Oil) has the highest value of the heat transfer rate followed by (CuO-EG). From the results achieved, the lowest thermal resistance is expected with the (CuO-Oil) base Nano fluid. But, there is no important difference in (Nu) for water, and EG but when the plot is zoomed in, there are small changes in (Nu) where oil-base Nano fluid has the highest (Nu) value, water is the least. Therefore, the presence of a (CuO) nanoparticle in oil could greatly enhance the cooling of the enclosure compared with other types of base fluids studied; due to its have the high Prandtl number base fluids. Thus, enclosure with high Prandtl number base Nano fluid can be removed high heat flux.

### **CONCLUSION :-**

The current investigation numerically studies the buoyancy-driven heat transfer convection enhancement of three basic fluids (water, EG, oil) based (CuO) Nano fluid in differentially heated enclosure for two cases of boundary conditions (isothermal , and linearly varying) temperature. The achieved computations can be concluding an important point such as:

- I.** Both increasing in the value of Rayleigh number and solid volume fraction leads to increase the equivalent average Nusselt number.
- II.** The averaged heat transfer rate for all types of base Nano fluid that were tested in this study increases with the increase of the Prandtl number.
- III.** The type of basic fluids of Nano fluid is a main factor for heat transfer enhancement. The highest values are found when using (oil) with nanoparticles. Though, CuO-oil mixture has a better heat transfer enhancement as compared to water, and EG mixture.
- IV.** The percentage enhancement in heat transfer with (0.1) solid volume fraction of (CuO) particles based with different basic fluids such as (water, EG, or oil) increases (26.7%, 28.8%, and 32.94%) respectively for ( $Ra=10^3$ ) as compared to the base fluid. The percentage Heat transfer enhancement of Nano fluid with (0.1) solid volume fraction of (CuO) particles based with different basic fluids such as (water, EG, or oil) increases (23.6%, 24.97%, and 30.2%) respectively for ( $Ra=10^6$ ) as compared to the base fluid. Therefore, the choice of basic fluid is very important in the convective heat transfer application .

**Table (1):** Thermo-physical properties of basic fluids and nanoparticles

Physical properties	Base fluid			Nanoparticles
	Water	Ethylene glycol	Oil	CuO
$\rho$ (kg/m <sup>3</sup> )	997.1	1116	888.23	6500
$C_p$ (J/kg.K)	4179	2382	1880.3	540
$k$ (W/m.K)	0.613	0.249	0.145	18
$\beta$ (K <sup>-1</sup> )	0.00021	0.00065	0.00845	0.0000085

**Table (2):** Grid independency results (Pr = 6.7, Ra=10<sup>4</sup>).

$M \times N$	51 × 51	61 × 61	71 × 71	81 × 81	91 × 91
$Nu$	2.183	2.198	2.209	2.216	2.219

**Table (3):** The average Nusselt number of the isothermal hot wall for the first test code, comparison between the present results and the results of other investigators.

	Ra=10 <sup>3</sup>	Ra=10 <sup>4</sup>	Ra=10 <sup>5</sup>	Ra=10 <sup>6</sup>
Present study	1.101	2.216	4.536	8.686
Markatos and Pericleous (1984)	1.108	2.201	4.430	8.754
Fusegi et al. (1991)	1.105	2.302	4.646	9.012
Khanafer et al. (2003)	1.118	2.245	4.522	8.826
Tiwari and Das (2007)	1.0871	2.195	4.450	8.803
K.C.Lin, A. Violi (2010)	1.118	2.243	4.511	8.758
G.A. Sheikhzadeh et al. (2011)	1.148	2.311	4.651	9.010

**Table (4):** Effects of solid volume fraction on  $(Nu)_{average}$  and its relative increase percentage,

$$[\varepsilon = \frac{Nu_{\phi} - Nu_{\phi=0\%}}{Nu_{\phi=0\%}} \times 100\%], \text{ for (CuO-H}_2\text{O) nanofluid, at different Ra for two cases.}$$

case		$\phi=0\%$	$\phi=2\%$	$\phi=4\%$	$\phi=6\%$	$\phi=8\%$	$\phi=0.1$		
c 1. isothermal	Ra=10 <sup>3</sup>	Nu	1.101	1.154	1.213	1.273	1.334	1.395	
		increase%	0	4.8	10.2	15.6	21.16	26.7	
	Ra=10 <sup>4</sup>	Nu	2.216	2.312	2.424	2.533	2.632	2.734	
		increase%	0	4.3	9.4	14.3	18.8	23.4	
	Ra=10 <sup>5</sup>	Nu	4.536	4.692	4.922	5.146	5.365	5.579	
		increase%	0	3.4	8.5	13.4	18.3	23	
	Ra=10 <sup>6</sup>	Nu	8.686	9.07	9.522	10.008	10.44	10.736	
		increase%	0	4.4	9.6	15.2	20.2	23.6	
	c2. linearly varying temperature	Ra=10 <sup>3</sup>	Nu	0.545	0.575	0.605	0.636	0.667	0.698
			increase%	0	5.5	11	16.7	22.4	28.07
Ra=10 <sup>4</sup>		Nu	1.03	1.084	1.136	1.187	1.236	1.285	
		increase%	0	5.2	10.3	15.2	20	24.76	
Ra=10 <sup>5</sup>		Nu	2.169	2.285	2.396	2.505	2.61	2.712	
		increase%	0	5.35	10.46	15.5	20.3	25	
Ra=10 <sup>6</sup>		Nu	4.15	4.372	4.587	4.782	5.009	5.213	
		increase%	0	5.35	10.5	15.2	20.7	25.6	

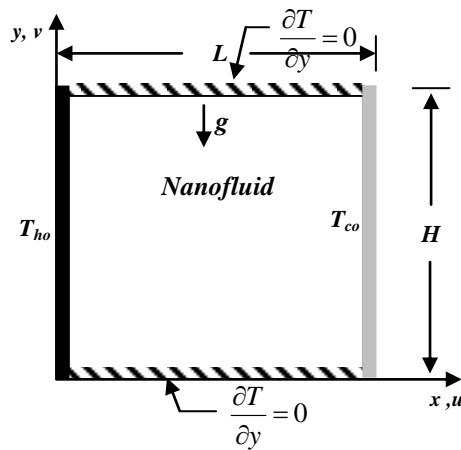


**Fig.(1):** Schematic for the physical model of the problem.

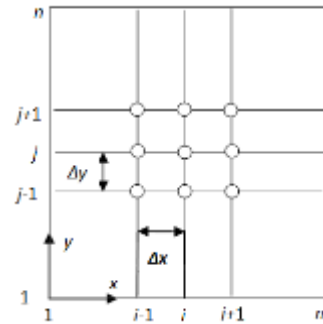


**Fig.(2):** Uniform grid distribution for two dimensional discretized domain.

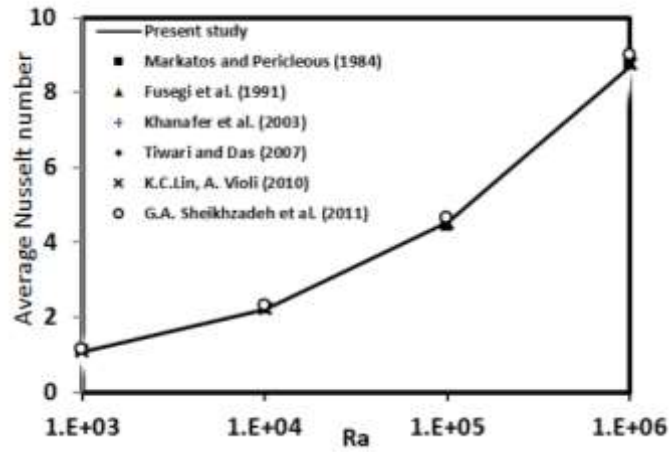


**Fig. (3):** Comparison between present work and other published work for the average Nusselt number versus (Ra) number.

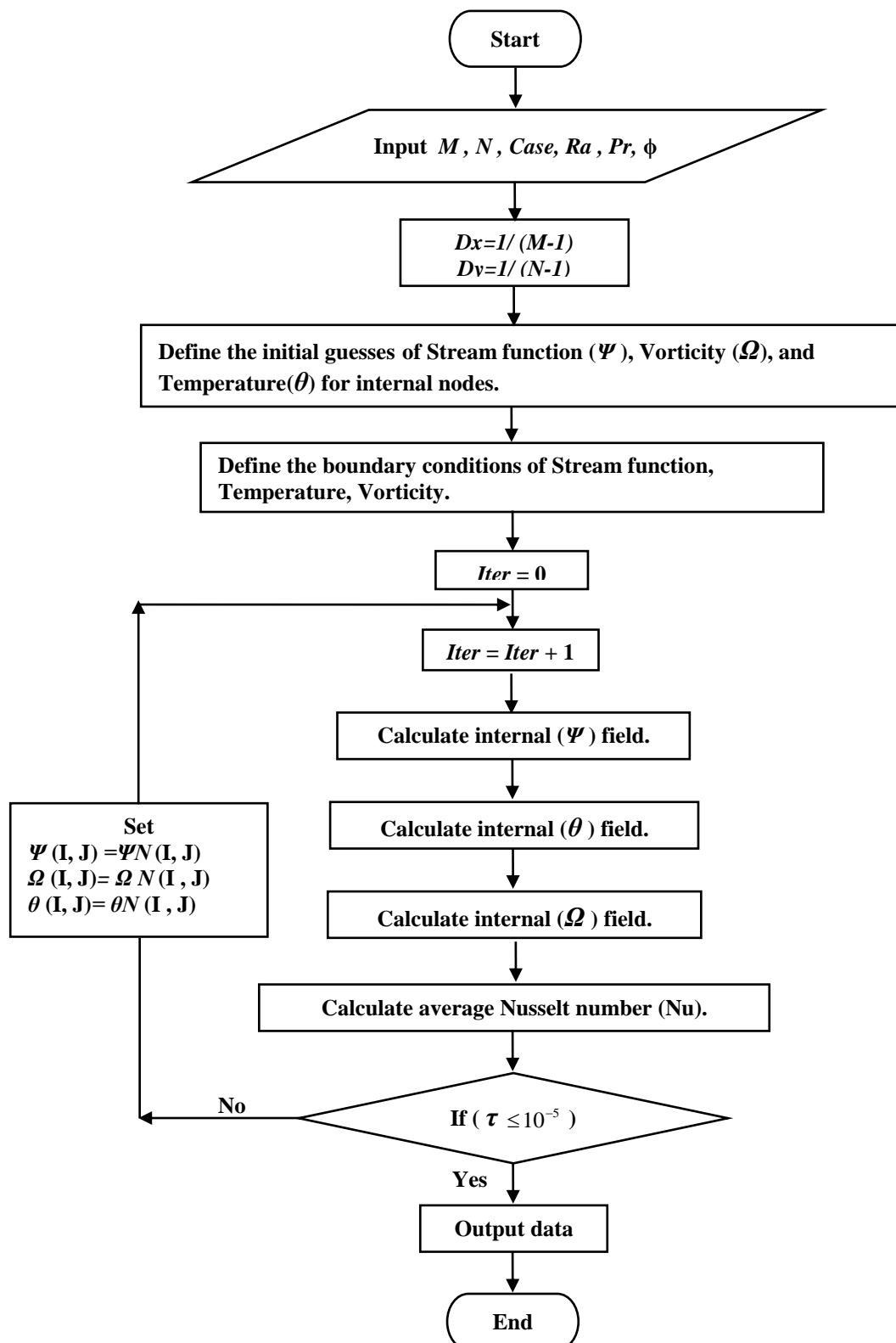
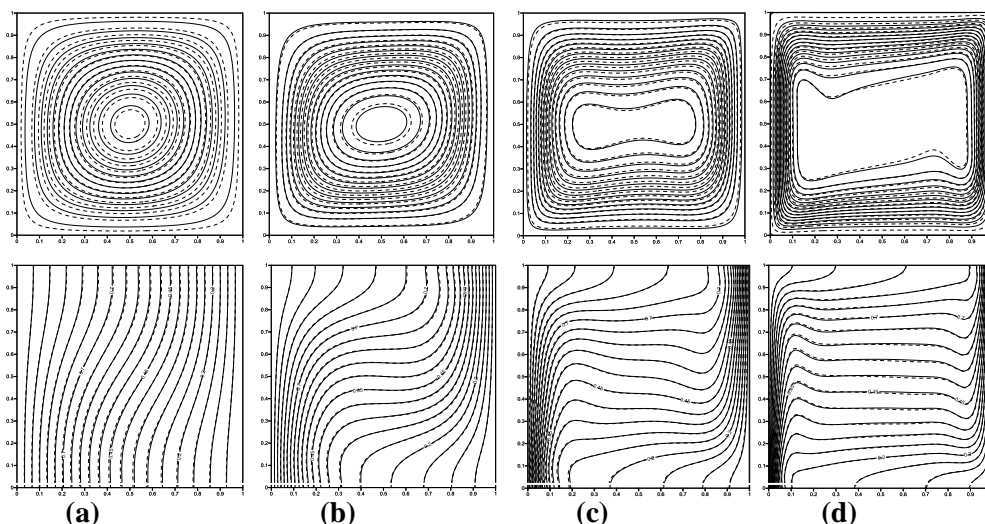
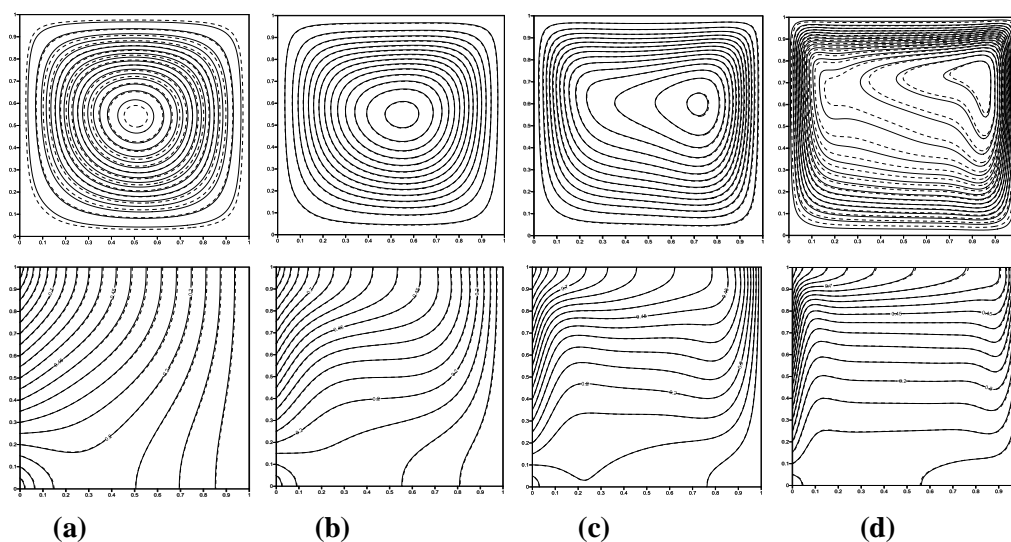


Fig. (4): Flow chart for computer program.



**Fig.(5):** Streamlines (on the top) and Isotherms (on the bottom) for Nano fluids ( - - - ) at  $\phi=4\%$  , pure fluid ( — ) case1 : (a)  $Ra=10^3$  ( $\Psi_{min}=-1.36$ ), (b)  $Ra=10^4$  ( $\Psi_{min}=-5.8$ ), (c)  $Ra=10^5$  ( $\Psi_{min}=-12.5$ ), and (d)  $Ra=10^6$  ( $\Psi_{min}=-20$ ).



**Fig.(6):** Streamlines (on the top) and Isotherms (on the bottom) for Nano fluids ( - - - ) at  $\phi=4\%$  , pure fluid ( — ) case2 : (a)  $Ra=10^3$  ( $\Psi_{min}=-0.71$ ), (b)  $Ra=10^4$  ( $\Psi_{min}=-3.6$ ), (c)  $Ra=10^5$  ( $\Psi_{min}=-8$ ), and (d)  $Ra=10^6$  ( $\Psi_{min}=-12.5$ ).

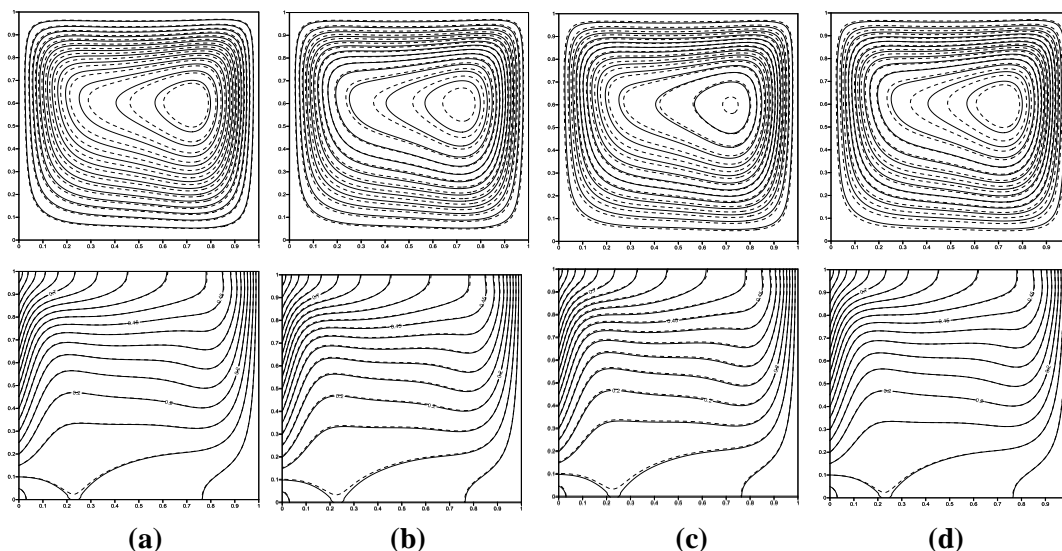


**Fig.( 7):** Streamlines (on the top) and Isotherms (on the bottom) for Nano fluids ( - - - ) at  $Ra=10^5$ , pure fluid ( — ) , case2 : (a)  $\phi=2.5\%$  ( $\Psi_{min}=-7.5$ ), (b)  $\phi=5\%$  ( $\Psi_{min}=-8$ ), (c)  $\phi=7.5\%$  ( $\Psi_{min}=-8.5$ ), and (d)  $\phi=0.1$  ( $\Psi_{min}=-9$ ).

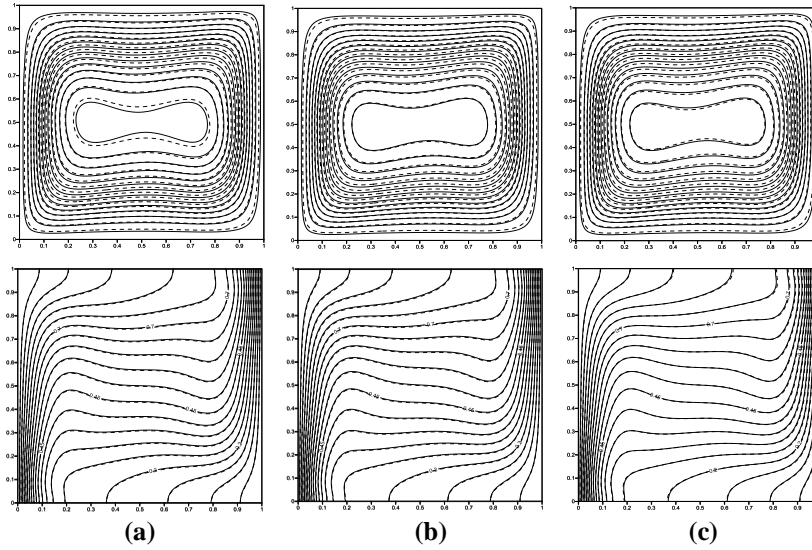


**Fig.( 8):** Streamlines (on the top) and Isotherms (on the bottom) for Nano fluids ( - - - ) , pure fluid ( — ) at  $Ra=10^5$  , and  $\phi=4\%$  for case 1 : (a) CuO-H2O , (b) CuO-EG , and (c) CuO-Oil .

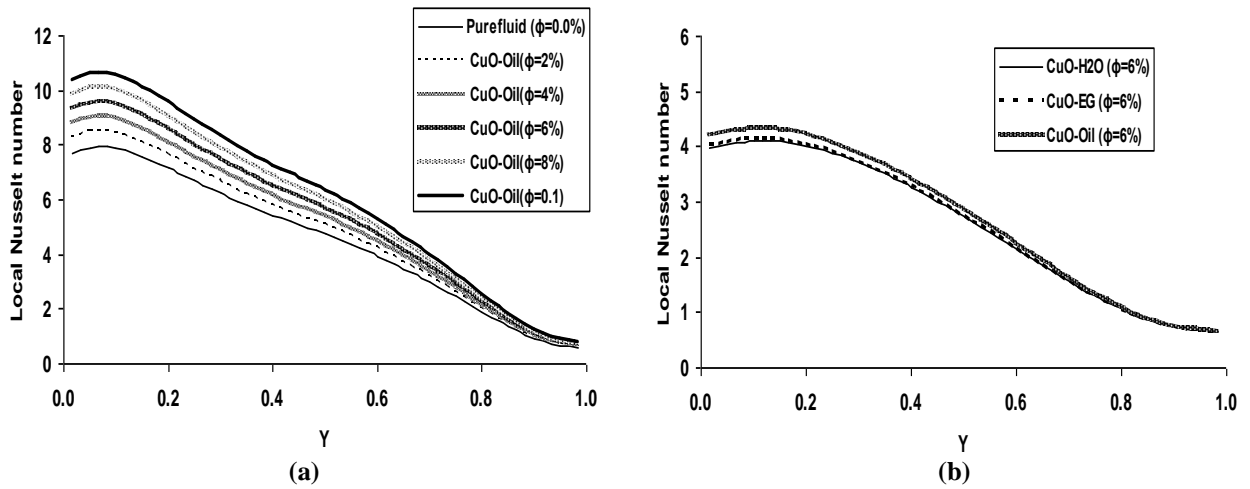


**Fig. (9):** Variation of local Nusselt number along the heated wall, case1: (a) for different solid volume fraction of CuO-Oil at  $Ra = 10^5$  , and (b) for CuO- with various basic fluid at  $Ra = 10^4$  .

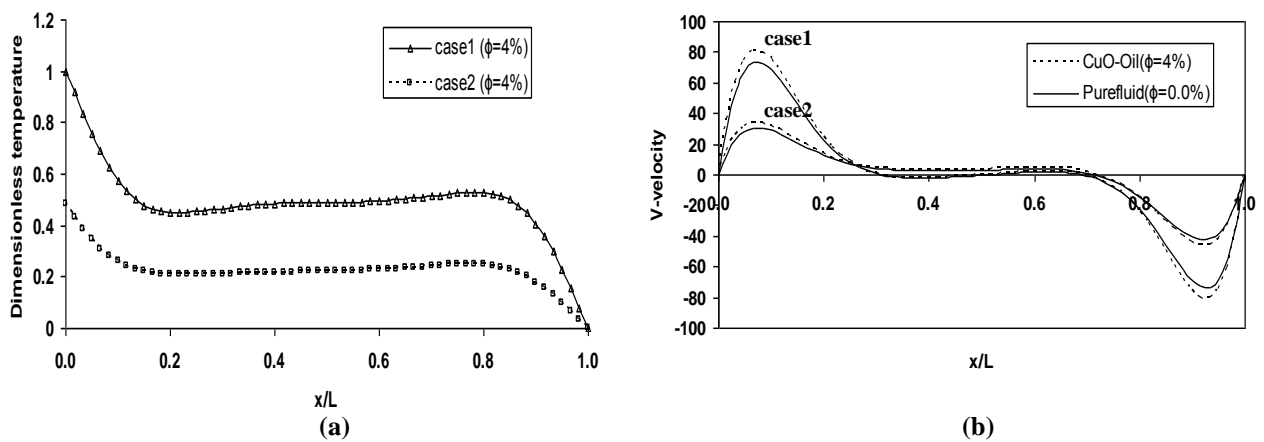


**Fig. (10):** Comparison of the isotherm and velocity profiles between nanofluid and pure fluid for: (a)  $Ra = 10^4$  , and (b)  $Ra = 10^5$  .

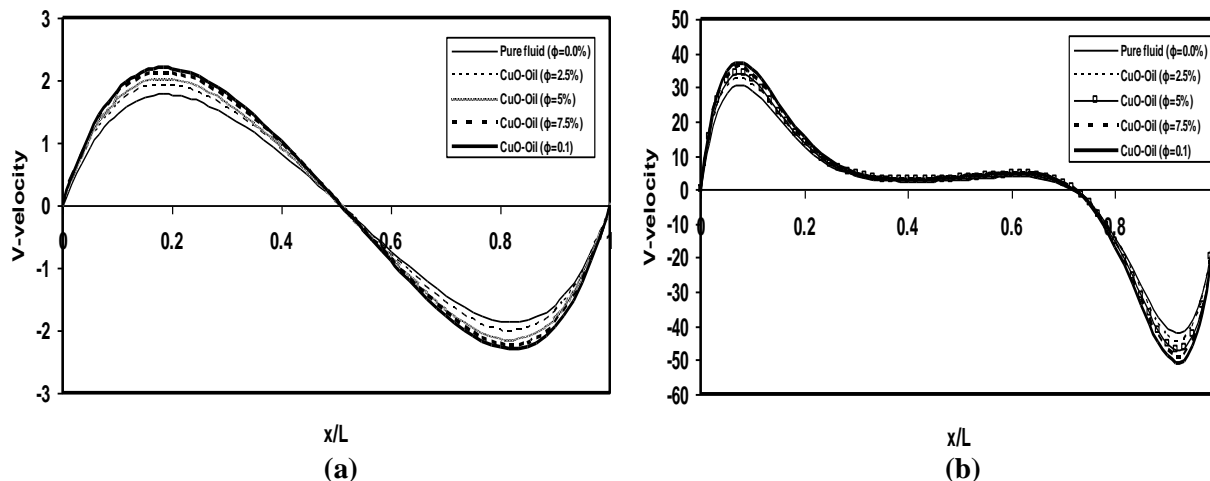


Fig. (11): Variation of V-velocity along the mid-span of the enclosure for case (a)  $Ra = 10^3$ , and (b)  $Ra = 10^5$ .

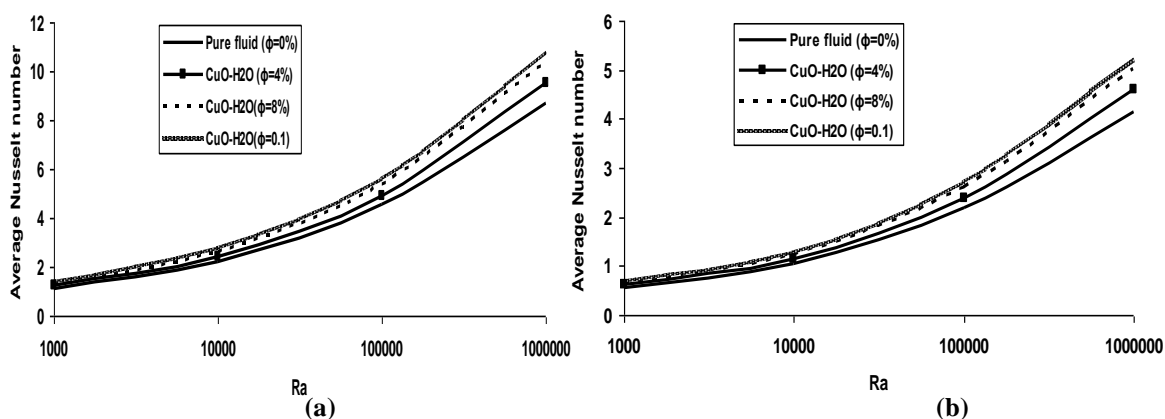


Fig. (12): Comparison of average Nusselt numbers with (Ra) numbers for different solid volume fraction of CuO-H2O Nano fluid: (a) isothermal boundary condition, (b) linearly varying boundary condition.

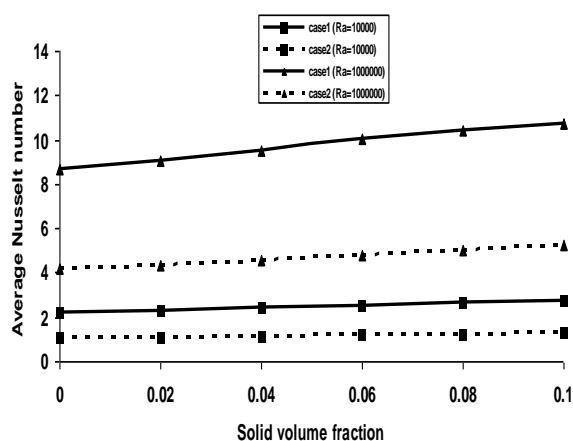


Fig. (13): Comparison of average Nusselt numbers with solid volume fraction of CuO-H2O Nano fluid for different (Ra) numbers, case1, and case2.

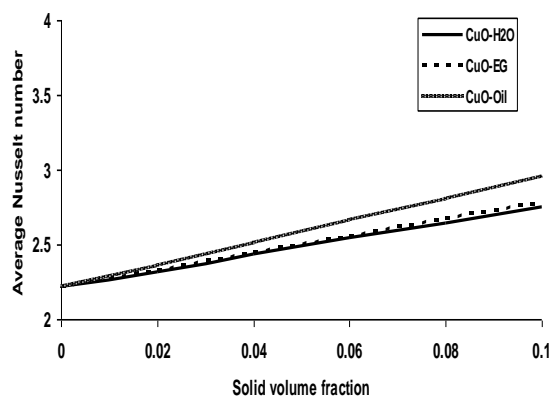


Fig. (14): Variation of average Nusselt numbers with solid volume fraction of CuO-with different basic fluids, case1 at  $Ra = 10^4$ .

## REFERENCES :-

Abu-Nada, E., Oztop, H.F., (2009) "Effects of inclination angle on natural convection in enclosures filled with Cu–water Nano fluid." *Int. J. Heat Fluid Flow* 30, pp.669–678.

Aminossadatia S.M., Ghasemi B., (2009) "Natural convection cooling of a localized heat source at the bottom of a Nano fluid-filled enclosure." *European Journal of Mechanics B/Fluid* 28, pp.630–640.

Ayad M. Salman, (2011)"An Investigation of Natural Convection Heat Transfer in a Square Enclosure Filled with Nano fluid" *Eng. & Tech. Journal*, vol.29, No.12, pp.2346-2363.

Brinkman H.C., (1952) "The viscosity of concentrated suspensions and solution", *Journal of Chemical Physics* 20, pp.571–581.

Fusegi T. et al., (1991) "A numerical study of three dimensional natural convection in a differentially heated cubical enclosure", *Int. J. Heat Mass Transfer* 34, pp.1543–1557.

Ho C.J., M.W. Chen, Z.W. Li, (2008) "Numerical simulation of natural convection of Nano fluid in a square enclosure: effects due to uncertainties of viscosity and thermal conductivity." *Int. J. Heat and Mass Transfer* 51, pp.4506–4516.

Hwang, K.S., Lee, Ji-Hwan, Jang, S.P., (2007) "Buoyancy-driven heat transfer of water based Al<sub>2</sub>O<sub>3</sub> Nano fluids in a rectangular cavity." *Int. J. Heat Mass Transfer* 50, pp.4003–4010.

Jou, R.Y., Tzeng, S.C., (2006) "Numerical research of nature convective heat transfer enhancement filled with Nano fluids in rectangular enclosures." *Int. Comm. Heat Mass Transfer* 33, pp.727–736.

Khanafar, K., Vafai, K., Lightstone, M., (2003) "Buoyancy-driven heat transfer enhancement in a two-dimensional enclosure utilizing Nano fluids." *Int. J. Heat Mass Transfer* 46, pp.3639–3653.

Lin K.C., A. Violi, (2010) "Natural convection heat transfer of Nano fluids in a vertical cavity: Effects of non-uniform particle diameter and temperature on thermal conductivity" *Int. J. Heat and Fluid Flow* 31, pp.236–245.

Markatos N.C., Pericleous K.A., (1984) "Laminar and turbulent natural convection in an enclosed cavity", *Int. J. Heat Mass Transfer* 27, pp. 772–775.

Najdat N. A., (1987) "Laminar Flow Separation in Constructed Channel", Ph.D. Thesis, Michigan State University.

Sheikhzadeh G.A. et al. (2011)" Natural convection of Cu–water Nano fluid in a cavity with partially active side walls" / *European Journal of Mechanics B/Fluids* 30, pp.166–176.

Tiwari, R.K., Das, M.K., (2007) "Heat transfer augmentation in a two-sided lid-driven differentially heated square cavity utilizing Nano fluids." *Int. J. Heat Mass Transfer* 50, pp.2002–2018.

Xuan Y., Q. Li,(2003) "Investigation on convective heat transfer and flow features of Nano fluids." *Journal of Heat Transfer* 125, pp.151–155.